# **Inorganic Chemistry**

pubs.acs.org/IC Article

### Halogen Bonding and/or Covalent Bond: Analogy of 3c-4e N···I···X (X = Cl, Br, I, and N) Interactions in Neutral, Cationic, and Anionic **Complexes**

Emmanuel Adeniyi, Favour E. Odubo, Matthias Zeller, Yury V. Torubaev, and Sergiy V. Rosokha\*



Cite This: Inorg. Chem. 2023, 62, 18239-18247



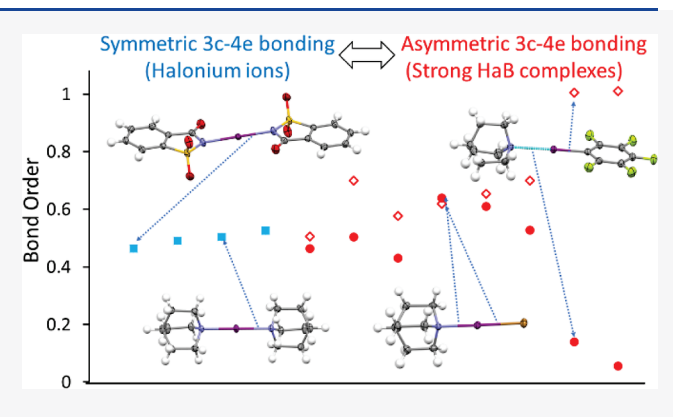
**ACCESS** 

III Metrics & More

Article Recommendations

Supporting Information

ABSTRACT: X-ray structural measurements and computational analysis demonstrated the similarity of the geometries and electronic structures of the X-I···N (X = Cl, Br, I, and N) bonding in strong halogen-bonded (HaB) complexes and in the anionic or cationic halonium ions. In particular, I···N bond lengths in the solid-state associations formed by strong HaB donors (e.g., I2, IBr, ICl, and N-iodosuccinimide) and acceptors (e.g., quinuclidine or pyridines) were in the same range of 2.3  $\pm$  0.1 Å as those in the halonium ions [e.g., the bis(quinuclidine)iodonium cation or the 1,1'-iodanylbis(pyrrolidine-2,5-dione) anion]. In all cases, bond lengths were much closer to those of the N-I covalent bond than to the van der Waals separations of these atoms. The strong N···I bonding in the HaB complexes led to a substantial charge transfer,



lengthening and weakening of the I···X bonds, and polarization of the HaB donors. As a result, the central iodine atoms in the strong HaB complexes bear partial positive charges akin to those in the halonium ions. The energies and Mayer bond orders for both N···I and I...X bonds in such associations are also comparable to those in the halonium ions. The similarity of the bonding in such complexes and in halonium ions was further supported by the analysis of electron densities and energies at bond critical (3, -1) points in the framework of the quantum theory of atoms in molecules and by the density overlap region indicator. Overall, all these data point out the analogy of the symmetric N···I···N bonding in the halonium ions and the asymmetric X···I···N bonding in the strong HaB complexes, as well as the weakly covalent character of these 3c-4e interactions.

#### 1. INTRODUCTION

Halogen bonding became a focal point of supramolecular chemistry during the last 20 years or so. 1-3 However, many associations that nowadays are considered halogen-bonded (HaB) complexes were extensively studied long before this term was defined by the IUPAC in 2013.4 Complexes between dihalogens or interhalogens and various electron-rich species represent an example of such systems.<sup>5</sup> In fact, the adduct formed by diiodine with ammonia was reported more than 200 years ago.6 Identification of complexes between diiodine and arenes in solutions by Benesi and Hildebrand and X-ray structural characterization of the association between dibromine and 1,4-dioxane (and other electron donors) in the solidstate by Hassel et al. led to the development of the Mulliken (charge-transfer) theory of molecular complexes and a flurry of studies in this area during the 1950s-1970s.7-12 The driving force of such associations was related to the interaction of the highest occupied molecular orbital (HOMO) of the electron donor (HaB acceptor) with the (antibonding) lowest unoccupied molecular orbital (LUMO) of the electron acceptors (HaB donor). The resulting orbitals of the complex contain contributions from the frontier orbitals of the donor and acceptor (Figure 1), which leads to ground-state charge transfer and the appearance of diagnostic charge-transfer bands in the absorption spectra. 10

In recent years, halogen bonding is most commonly been related to the electrostatic attraction of electron-rich species to areas of positive potential on the surfaces of covalently bonded halogen atoms.  $^{13}$  This  $\sigma$ -hole model of HaB complex formation is illustrated in Figure 2A.

Trihalide anions represent another association which are known for more than a century. 14 The bonding in these species was discussed by Pauling in 1940 and subsequently analyzed in detail by Rundle and Pimentel. 15-17 The simplified MO diagram of trihalides (Figure 1, right) indicates that it can be interpreted as the interaction of filled orbitals of two electron donors D (in this case, halide anions) with an empty orbital of

Received: August 15, 2023 Published: October 23, 2023





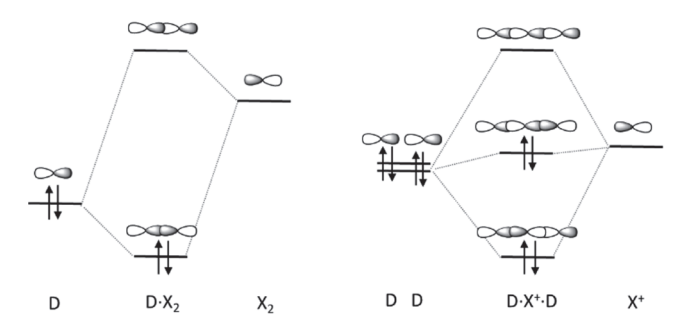


Figure 1. Simplified molecular-orbital diagrams of  $D \cdot X_2$  (left) and  $D \cdot X^+ \cdot D$  (right,  $D = X^-$  or a different nucleophile).



Figure 2. Electrostatic ( $\sigma$ -hole) model showing the attraction of electron-rich species (red) to the area of the positive potential (blue) on the surface of the halogen atom in halonium cations (A) and conventional HaB complexes (B).

an electron acceptor (here, a halonium cation). Such an interaction produces filled bonding and nonbonding orbitals and an empty antibonding orbital at the trihalide. With four electrons delocalized over three atoms, the interaction in these anions is frequently referred to as 3c–4e bonding. Similar orbital interactions take place in the systems in which terminal halides are replaced by other neutral or anionic electron donors, D (the Lewis bases). The charge of D together with the formally positive charge of the central halogen atom determines the overall (cationic or anionic) charge of the halonium ions.

The variety of applications of trihalides and halonium ions, from mediating electron transfer in solar cells to synthetic organic chemistry,  $^{18-23}$  led to a large number of experimental and computational studies.  $^{23-30}$  However, the nature of this bonding still remains a matter of debate. Besides weakly covalent 3c–4e bonding, it was sometimes referred to as a reversible or dynamic covalent bond or viewed as coordination bonding of I<sup>+</sup> with two Lewis bases. These complexes were also regarded as hypervalent species with an expanded octet to ten electrons. Following the electrostatic ( $\sigma$ -hole) model of the bonding in the conventional HaB complexes, the bonding in D–I<sup>+</sup>–D associations was also interpreted as an attraction of two Lewis bases to two  $\sigma$ -holes on the surface of I<sup>+</sup> cations (Figure 2A).  $^{31}$ 

It should be noted that the 3c–4e bonding in D–I<sup>+</sup>–D species is usually shorter and stronger than the conventional halogen bonds. Many recent studies showed, however, that complexes between strong HaB donors, e.g., diiodine or interhalogens, IX (X = I, Br, or Cl), and strong nucleophiles, e.g., 1,4-diazabicyclo[2.2.2]-octane (DABCO) are characterized by the very short I···N bonds of about 2.25–2.30 Å, which are close to that in the cationic or anionic associations comprising N–I<sup>+</sup>–N fragments [e.g., bis(1,4-diazabicyclo[2.2.2]octane)iodine(I), or 1,1'-iodanylbis-(pyrrolidine-2,5-dione)]. Computational analysis also demonstrated that many characteristics of the bonding in complexes of DABCO with IX are close to those in the trihalide anions. Similar short N–I distances were also observed in the complexes of some nucleophiles with N-iodosaccharin and N-iodosuccinimide.

previous publications suggested that the interaction in the strong HaB complexes (e.g., chlorine with phosphines) can also be described as 3c–4e bonding. 42–45 Still, a detailed comparison of the characteristics of such X–I···N halogen bonding vis-à-vis 3c–4e N···I···N interactions in the halonium ions is lacking. Thus, the goals of the current work are to clarify the relationship between these types of interactions and the nature of these bonds. Accordingly, we carried out an experimental and/or computational analysis of the HaB complexes formed by quinuclidine (QN) or pyridines with the strong HaB donors, e.g., I<sub>2</sub>, IBr, and ICl, or N-iodo-substituted succinimide or saccharine illustrated (together with their acronyms) in Scheme 1.

### Scheme 1. Structures and Acronyms of HaB Donors and Acceptors

Similar to DABCO, QN and pyridines are capable of forming strong HaB complexes or iodonium ions. 40,46,47 Due to the presence of only one nucleophilic nitrogen, they form 1:1 associations, which facilitate the comparison of the computational and experimental data. The juxtaposition of the characteristics of the complexes of QN or pyridine with the strong HaB donors with that of the typical halonium anions and cations, as well as of the weaker HaB complexes (such as that formed by QN with IPFB), allows elucidation of similarities and distinctions (if any) between the nature of interactions in these associations.

## 2. EXPERIMENTAL AND COMPUTATIONAL METHODS

**2.1. Materials.** Commercially available QN, iodopentafluorobenzene, *N*-iodosaccharine, diiodine, iodine monochloride, and iodine monobromide were used without additional purification.

The addition of a solution containing 1.0 mmol of ICl (163 mg) in hexane to a solution of 1.0 mmol of QN (111 mg) in hexane immediately produced a yellow precipitate in an essentially quantitative yield (267 mg). The precipitate was filtered, washed with hexane, and dissolved in acetonitrile. The clear yellow solution was cooled slowly to -35  $^{\circ}$ C and left at this temperature for several days. This resulted in the formation of pale-yellow rhombic plates of QN·ICl (1). Yield: 161 mg (59%). Mp: 185-188 °C (decomp). Elemental analysis (%): calcd for C<sub>7</sub>H<sub>13</sub>ClIN (273.54 g mol<sup>-1</sup>): C 30.74, H 4.79, N 5.12; found C 30.72, H 4.74, N 5.15. IR (ATR, cm<sup>-1</sup>): 2982, 2947, 2921, 2869, 1680, 1474, 1453, 1366, 1319, 1311, 1278, 1205, 1168, 1038, 982, 958, 902, 828, 780, 637. Crystals of QN· IBr (2) suitable for single-crystal X-ray structural measurements were obtained in a similar way by the interaction of 1.0 mmol of IBr (207 ng) with 1.0 mmol of QN (111 mg) in hexane, followed by the recrystallization of the pale yellow powder from acetonitrile. Yield: 179 mg (56%). Mp 176-179 °C (decomp). Elemental analysis (%): calcd for  $C_7H_{13}BrIN$  (318.00 g mol<sup>-1</sup>): C 26.44, H 4.12, N 4.40; found C, 26.48, H 4.28, N 4.25. IR (ATR, cm<sup>-1</sup>): 2978, 2943, 2919, 2867, 1472, 1452, 1364, 1318, 1311, 1277, 1204, 1167, 1043, 1018, 982, 900, 826, 776, 636. Colorless crystals of QN-IPFB (3) were obtained by slow evaporation of a hexane solution comprising a mixture of 1.0 mmol of IPFB (294 mg) and 1.0 mmol of QN (111 mg), followed by cooling to -35 °C. Yield: 270 mg (67%). Mp: 51-53 °C Elemental analysis (%): calcd for C<sub>13</sub>H<sub>13</sub>F<sub>5</sub>IN (405.15 g

mol<sup>-1</sup>): C 38.54, H 3.23, N 3.46; found C, 38.54, H 3.13, N 3.37. IR (ATR, cm<sup>-1</sup>): 2949, 2928, 2871, 1634, 1579, 1506, 1476, 1456, 1383, 1364, 1358, 1322, 1270, 1202, 1139, 1076, 1052, 1004, 990, 981, 968, 824, 803, 785, 775, 713. Mixing acetonitrile solutions of 0.50 mmol of QN (56 mg) and 0.50 mol (155 mg) of ISac and cooling the resulting solutions to -35 °C and keeping them at this temperature for several days afforded light yellow plates. X-ray analysis showed that they comprised [QN-I-QN]<sup>+</sup>[Sac-I-Sac]<sup>-</sup> (4) salt consisting of cationic bis(1,4-diazabicyclo[2.2.2]octane)-iodine(I) and anionic bis(1,1,3-trioxo-1,3-dihydro-2*H*-1,2-benzothiazol-2-yl)iodide counterparts. Yield: 107 mg (51%). Mp 174–176 °C. Elemental analysis (%): calcd for  $C_{28}H_{34}I_2N_4O_6S_2$  (840.53 g mol<sup>-1</sup>): C 40.01, H 4.08, N 6.67; found C, 40.12, H 4.11, N 6.63. IR (ATR, cm<sup>-1</sup>): 2955, 2930, 2874, 1678, 1592, 1482, 1458, 1371, 1353, 1334, 1278, 1325, 1169, 1158, 1133, 1125, 1058, 1018, 990, 953, 878, 832, 786, 772, 748, 707, 675, 654.

**2.2.** X-ray Crystallographic Analysis. The cell determination and the intensity data collection were carried out with a Bruker AXS Quest diffractometer equipped with graphite-monochromated Mo K $\alpha$  radiation (0.71070 Å). The data were collected by the standard  $\varphi-\omega$  scan techniques and reduced using SAINT v8.37A. SADABS was used for scaling and absorption correction. SaINT v8.37A to structures were solved by direct methods and refined by full-matrix least-squares against  $F^2$  using ShelXI with the ShelXle GUI. Sol.51 Non-hydrogen atoms were refined with anisotropic thermal parameters. All hydrogen atoms were geometrically fixed and refined using a riding model. Crystallographic, data collection, and structure refinement details are listed in Table S1 in the Supporting Information.

2.3. Computations. The geometries of the complexes were optimized without constraints via M062X/def2tzvpp calculations using the Gaussian 09 suite of programs. 52-54 For comparison with the experimental data, calculations were done in dichloromethane (since this moderately polar solvent is well suited for modeling ionic salts and polar substances in a solid state) using a polarizable continuum model.<sup>55</sup> An earlier analysis demonstrated that intermolecular HaB associations are well-modeled using this method. 56,57 The energies and atomic coordinates of the optimized species are listed in the Supporting Information. Binding energies,  $\Delta E_{\rm h}$  were determined as  $\Delta E_b = E_C - (E_A + E_B)$ , where  $E_C$ ,  $E_A$ , and  $E_B$  are sums of the electronic and ZPE of the optimized complex and its counterparts (A and B). In particular, the  $\Delta E_b(N - I)$  in the HaB complexes were evaluated with A = QN or pyridine and B = HaB donor (ICl, IBr, etc.,), and  $\Delta E_b(\text{I} \cdot \cdot \cdot \text{X})$  was found with A = QN-I<sup>+</sup> or Pyr-I+ cation and B is an anionic residue of the HaB donor (Cl-, Br-, etc.,).  $\Delta E_b(N \cdot \cdot \cdot I)$  values in the halonium ion were determined with iodine-containing (e.g., QN-I+ or ISac) and iodo-free fragments (e.g., QN or Sac-) as A and B. Since the formation of the complex is accompanied by a distortion of the reactants, the binding energy represents a combination of preparation (distortion) energy,  $E_{\text{prep}}$ , and interaction energy between distorted fragments,  $\Delta E_{\rm int}$ . Charge transfer values,  $\Delta q$ , were estimated *via* natural bond orbital (NBO)<sup>3</sup> and quantum theory of atoms in molecules (QTAIM) calculations.<sup>59</sup> QTAIM, the density overlap region indicator (DORI),<sup>60</sup> and the Mayer bond order (MBO)<sup>61,62</sup> analyses were performed with Multiwfn and visualized using VMD programs<sup>63,64</sup> (note that these analyses were performed using both optimized geometries and experimental geometries extracted from the X-ray structures, and the results obtained for a certain complex were similar). Intermolecular interaction energy calculation in the solid-state associations was performed using CrystalExplorer 21.5 (TONTO and B3LYP-DGDZVP),<sup>65</sup> using experimental crystal geometries from the X-ray structures. This method was developed for evaluation of the interaction energies in the solid-state material, and analysis of its performance showed that its results were close (with a mean absolute error of 0.7 kJ mol<sup>-1</sup>) to the counterpoise-corrected B3LYP-D2 interaction energies computed with a mixed basis set [DGDZVP on second-row transition metals and 6-31G(d,p) on all other atoms].<sup>66</sup>

#### 3. RESULTS AND DISCUSSION

3.1. X-ray Structural Characterization of the Solid-State Associations. Mixing hexane solutions containing equimolar quantities of QN and ICl or IBr resulted in the immediate formation of a yellow precipitate. Dissolution of these precipitates in acetonitrile and slow cooling of the resulting solutions to -35 °C produced rhombic plates suitable for X-ray crystallographic analysis. They comprised the 1:1 HaB complexes, as illustrated in Figure 3.

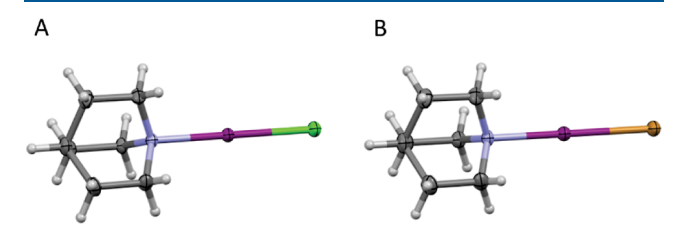


Figure 3. X-ray structures of the (A) QN·ICl (1) and (B) QN·IBr (2) complexes. Color code: dark gray—carbon, light gray—hydrogen, blue—nitrogen, magenta—iodine, green—chlorine, and brown—bromine.

These associations (and the complex of QN with  $I_2$  which was reported earlier by Rissanen *et al.*<sup>46</sup>) are characterized by almost linear halogen X–I···N bonds, which were slightly shorter than the corresponding distances in the isomorphic associations with DABCO (Table 1).

Table 1. Selected Characteristics of the Solid-State Complexes

complex	$d_{\mathbf{N}\cdots\mathbf{\nu}}$ Å	$d_{\text{I}\cdots \text{X}}$ , Å	E, a kcal/mol	structure
QN·ICl	2.268(3)	2.5891(8)	23.7	this work (1)
QN∙IBr	2.299(3)	2.7195(5)	20.2	this work (2)
$QN \cdot I_2$	2.351 <sup>b</sup>	2.869 <sup>b</sup>	15.2	IWABUG <sup>b</sup>
QN·IPFB	2.6859(11)	2.1306(13)	10.4	this work (3)
QN·IBEN	2.930 <sup>c</sup>	2.109 <sup>c</sup>	5.5	$INAJEP^c$
QN-I-Sim	$2.370^{d}$	$2.185^{d}$	19.4	IBOZOS <sup>d</sup>
Pyr-ISac	2.279 <sup>e</sup>	2.254 <sup>e</sup>	16.0	MUGDAU <sup>e</sup>
Pyr-ICl	2.284 <sup>f</sup>	$2.523^{f}$	14.6	PYRIIC11 <sup>f</sup>
Pyr-IBr <sup>f,g</sup>	2.304 <sup>f</sup>	$2.653^{f}$	11.4	PYIOBR03 <sup>f</sup>
Pyr-I <sub>2</sub>	2.425	2.804	8.0	VUHDIN <sup>h</sup>
QN-I-QN <sup>+i</sup>	2.3034(14)			this work (4)
Sac-I-Sac <sup>-j</sup>	2.2467(15)			this work (4)
Sim-I-Sim <sup>-k</sup>	$2.244/2.264^{i}$			YUNPUV <sup>k</sup>
Pyr-I-Pyr <sup>+1</sup>	2.259 <sup>j</sup>			CICQIQ <sup>1</sup>

<sup>a</sup>Interaction energy between N and I in the solid-state HaB complexes (calculated using CrystalExplorer<sup>65</sup>), see Table S3 in the Supporting Information for details and energy decomposition analysis. <sup>b</sup>Ref 46. <sup>c</sup>Ref 67. <sup>d</sup>Ref 47. <sup>e</sup>Pyr = pyridine, ref 68. <sup>f</sup>Ref 69. <sup>g</sup>Ref 70. <sup>h</sup>Ref 71. <sup>i</sup>Centrosymmetric cation in 4. <sup>f</sup>Centrosymmetric anion in 4. <sup>k</sup>Noncentrosymmetric anion, salt with t-Bu<sub>4</sub>N<sup>+</sup>, ref 37. <sup>l</sup>Salt with PF<sub>6</sub><sup>-</sup>, ref 72.

Their I···N bond lengths decrease in the order  $I_2 > IBr > ICl$ , which corresponds to the increases of the maximum electrostatic potential on the surface of iodine in the IX molecules. The N···I interaction energies in these solid-state associations (which were calculated using CrystalExplorer of increase in the same order. It is also noticeable that strong halogen I···N bonding led to about a 10% increase of the I–X bond length as

compared to the individual molecules (2.321, 2.469, and 2.665 Å in ICl, IBr, and  $I_2$ , respectively).<sup>35</sup>

*N*-Iodo-substituted saccharine and succinimide molecules represent another type of very strong HaB donor. For example, the reported earlier associations of ISim with QN are characterized by the I···N bond length of 2.370 Å. <sup>47</sup> Interaction N···I energy in this complex is comparable to that in complexes with I<sub>2</sub> (Table 1). Our attempts to crystallize associations of ISac with QN (see Experimental and Computational Methods Section for details) resulted in the formation of the product of halogen transfer, *i.e.*, the salt (4) of the centrosymmetric QN-I-QN<sup>+</sup> cations and Sac-I-Sac<sup>-</sup> anions (Figure 4). The interatomic I···N separations in the cationic

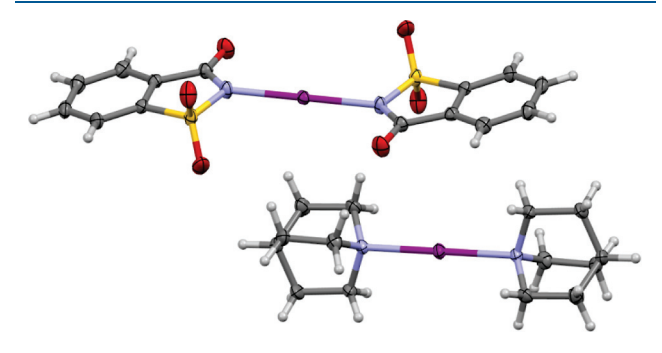


Figure 4. X-ray structure of the salt (4) showing cationic and anionic associations formed by the N···I···N interaction. Color code: dark gray—carbon, light gray—hydrogen, blue—nitrogen, magenta—iodine, red—oxygen, and yellow—sulfur.

and anionic counterparts were close to those in the HaB complexes of QN with interhalogens, as well as those in the reported complexes of ISac with 4-aminopyridine or pyridine,  $^{40,68}_{\phantom{0}}$  and in the halonium Pyr-I-Pyr $^{+}_{\phantom{0}}$  association (Table 1).  $^{72}_{\phantom{0}}$ 

The colorless blocks of the cocrystals of QN with IPFB (see Experimental and Computational Methods for details of their preparation) comprised 1:1 HaB complexes (Figure 5).

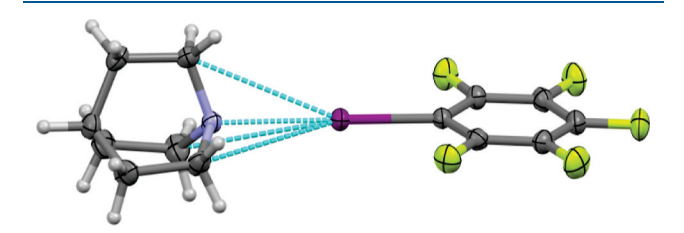


Figure 5. X-ray structure of the halogen-bonded complex of QN with IPFB (3). Color code: dark gray—carbon, light gray—hydrogen, blue—nitrogen, magenta—iodine, and lime—fluorine.

The I···N separation of 2.686 Å in this association was 24% shorter than the sum of the van der Waals radii of iodine and nitrogen. Besides the I···N bond length, the I···C distances were also shorter than the van der Waals separations. It should be noted in this respect that a search of the Cambridge Crystallographic Database showed that (close to linear) I···N separations are observed most frequently in the 2.70–2.95 Å range (Figure S1 in the Supporting Information). Thus, the I···N bond in the complex of QN with IPFB is shorter than the most typical I···N HaB lengths. In fact, even a reported complex of QN with the weak HaB donor, iodobenzene (IBEN), is characterized by an I···N separation of 2.930 Å,

which is 17% shorter than the van der Waals contacts (Table 1). Most notably, the N···I separations in the associations of QN with the strong HaB donors, such as interhalogens or N-iodosuccinimide, are in the same range of  $2.3 \pm 0.1$  Å as that found for the cationic or anionic halonium ions. Similar short bond lengths (about 1-2% longer than those in the corresponding associations with QN) were also observed in the complexes of the same HaB donors with pyridines. <sup>69-71</sup> To further compare bonding in the halonium ions with that in the complexes of different HaB donors with QN and pyridine molecules, we carried out quantum-chemical computations of these systems as follows.

**3.2. Computational Analysis of the Complexes.** To ensure that the bonding characteristics are determined by the intrinsic properties of the interacting species, the analysis of the bonding in the solid-state associations (which could be affected by the crystal forces) was accompanied by the consideration of fully optimized complexes. The optimizations were carried out using M062X/def2tzvpp computations (earlier works showed that this method produces excellent geometries and energies of HaB complexes at a reasonable computational cost). S55–S7 Binding energies and N···I and I···X bond lengths of the HaB complexes resulting from these calculations are listed in Table 2 (note that N···I···X angles in all calculated complexes were very close to 180°; see Table S2 in the Supporting Information).

Table 2. Calculated Bond Length and Energies of the Complexes<sup>a</sup>

complex	$\Delta E_{\rm b}$ , a kcal/mol		d, Å	
	N-I	I–X	N-I	I–X
QN·ICl	-24.0	-34.6	2.309	2.522
QN·IBr	-22.0	-32.0	2.320	2.676
$QN \cdot I_2$	-16.7	-31.1	2.368	2.838
QN·IPFB	-8.3	-66.6	2.700	2.115
QN·IBEN	-4.6	-100.0	2.930	2.107
QN-ISim	-17.2	-43.7	2.399	2.143
QN·ISac	-22.5	-31.4	2.310	2.212
Pyr·ISac	-15.7	-35.7	2.342	2.165
Pyr·ICl	-16.8	-38.5	2.327	2.480
Pyr∙IBr	-14.6	-35.8	2.346	2.523
$Pyr \cdot I_2$	-9.8	-35.4	2.432	3.779
$QN-I-QN^+$	-29.1		2.285	
Pyr-I-Pyr <sup>+</sup>	-24.7		2.252	
Sac-I-Sac	-18.2		2.245	
Suc-I-Suc	-20.8		2.244	

<sup>a</sup>From M062X/def2tzvpp calculations (PCM, CH<sub>2</sub>Cl<sub>2</sub>), see the energies and atomic coordinates of the complexes and their counterparts in the Supporting Information.

Comparison with the data in Table 1 reveals that the properties of the optimized complexes are close to those of the solid-state associations. In accordance with the solid state, the complexes with pyridine are somewhat weaker than the corresponding associations with QN. The linear dependence of the calculated and experimental I···N bond length is characterized by an  $R^2$  or 0.99 and a coefficient of 1.00 (Figure S2 in the Supporting Information), and the average difference between these values was less than 0.01 Å. The average difference of binding energies in the calculated and experimental HaB complexes was less than 0.5 kcal/mol. This confirms that the characteristics of the solid-state

associations obtained from the X-ray structural analysis are indeed determined by the intrinsic nature of these complexes and they are not affected substantially by crystal forces. It also verified the reliability of the M062X/def2tzvpp calculations in the modeling of such complexes.

Specifically, the I···N bond lengths and binding energies in the optimized HaB complexes of QN (or Pyr) with the strong HaB donors (IX, Isac, or ISim molecules) are in the same range as those in the cationic and anionic halonium complexes. It is also noticeable that in the strong HaB complexes, the I···N bond strengths are only about 1.5–2 times weaker than those of the corresponding I···X bonds. In comparison, the complexes with the weaker (IPFB and IBEN) HaB donors are characterized by I···N binding energies, which are about 8 and 21 times lower than the corresponding I···C bond (heterolytic) dissociation energies, and they are much lower than those in the halonium cations.

The similarity between the very strong HaB complexes and halonium ions is supported by the analysis of the charge distribution in all of these associations. Indeed, the formation of HaB complexes is accompanied by a considerable charge transfer from the QN to the HaB donor (of about 0.3e, see Table S4 in the Supporting Information). It also leads to a substantial polarization of the HaB donor. As a result, the X (or N) atoms in the HaB donor parts of the complexes are characterized by negative charges (Table S4 in the Supporting Information). The central iodine atoms are positively charged and their values in the strong complexes are close to those in the iodonium ions (Figure 6).

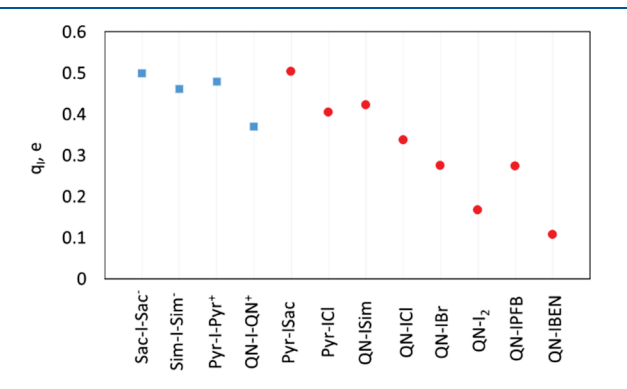


**Figure 6.** Charge on the central iodine atom in iodonium ions (blue squares) and HaB complexes (red circles), see Table S4 in the Supporting Information for the numerical values.

The analogy of I···N bonding in the neutral HaB complexes and iodonium ions was confirmed using the MBO indices. These indices quantify the degrees of bonding based on partitions of the electron density. 61,62 They generate values that are consistent with the generally accepted bond orders in simple covalent bonds and provide valuable information about bonding in a variety of systems.<sup>62</sup> The MBO values for the I··· N bonds in the solid-state complexes with the strong HaB donors are in the 0.44-0.64 range, as compared to 0.50  $\pm$  0.04 found for the iodonium ions under study (Table S5 in the Supporting Information). The MBO values in the latter are consistent with the formal bond orders of 0.5 in the systems with two bonding and two nonbonding electrons forming two bonds [which is commonly determined as BO =  $(N_b - N_{ab})$ / 2n, where  $N_{\rm b}$  is the number of electrons in the bonding orbitals,  $N_{ab}$  is the number of electrons in the antibonding orbitals in Figure 1, right, and n is the number of bonds, *i.e.*, n = 2 for D–I<sup>+</sup>–D association]. It is also noticeable that MBO values for I···N bonds in the strong (solid-state) complexes are comparable to the corresponding values for I···X bonds (Figure 7). In comparison, the MBO values of the I···N bonds in the

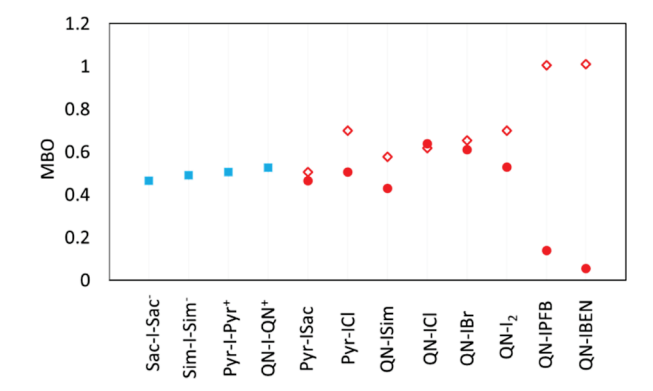


Figure 7. MBO for N···I bonds in halonium ions (blue squares) as well as  $I \cdot \cdot \cdot N$  (red circles) and  $I \cdot \cdot \cdot X$  (red rhombics) bonds in HaB complexes.

complexes with the weaker HaB donors are much lower than those found for the I···N bonds in the halonium ions and they are about ten times lower than those of the I···C bonds.

The parity of the strong bonding under study was affirmed *via* the analysis of the electron and energy densities at (3, -1) bond critical points (BCPs) using Bader's QTAIM.<sup>59</sup> QTAIM represents a powerful methodology for the classification and quantification of chemical bonding based on the topology of the electron densities and energies.<sup>75–81</sup> The majority of relevant previous studies were focused on hydrogen bonding, which is arguably the most important and well-studied supramolecular interaction.<sup>75,76</sup> Subsequently, they were extended to halogen and chalcogen-bonded systems.<sup>77–81</sup> Based on the topological and energetic properties of the electron density distribution, these works assigned three characteristic regions representing different interaction states, *i.e.*, limiting pure closed-shell (noncovalent), shared-shell (covalent) interactions, and the middle region, which involves the formation of the bonding molecular orbital.

Most commonly, QTAIM analyses are focused on the magnitude of density  $\rho(\mathbf{r})$ , the Laplacian,  $\nabla^2 \rho(\mathbf{r})$ , the kinetic energy and potential energy densities  $G(\mathbf{r})$  and  $V(\mathbf{r})$ , and the energy density  $H(\mathbf{r}) = G(\mathbf{r}) + V(\mathbf{r})$  at BCPs. These values for the HaB complexes and halonium ions are listed in Table S6 in the Supporting Information. The values of the electron density,  $\rho(\mathbf{r})$ , in the HaB complexes and halonium ions are illustrated in Figure 8.

A comparison of the data in Figure 8 with those in Tables 1 and 2 shows that the  $\rho(\mathbf{r})$  values vary in parallel to the changes in interaction energies. This confirmed earlier suggestions that electron densities at BCP represent a good indicator of the strength of bonding. It is thus notable that the electron densities at the BCPs at the N···I bond paths in the strong HaB complexes are in the same range (0.07-0.09 a.u.) as those in the halonium ions (which are all about 0.08 a.u.). Also, the values of  $\rho(\mathbf{r})$  at I···N bond paths in most complexes are close to or higher than those at the I···X bond paths, which confirms the comparable strength of these bonds. Importantly, all these values are closer to 0.1 a.u., which is characteristic of a covalent bond, than to 0.01 a.u., which is typical for intermolecular

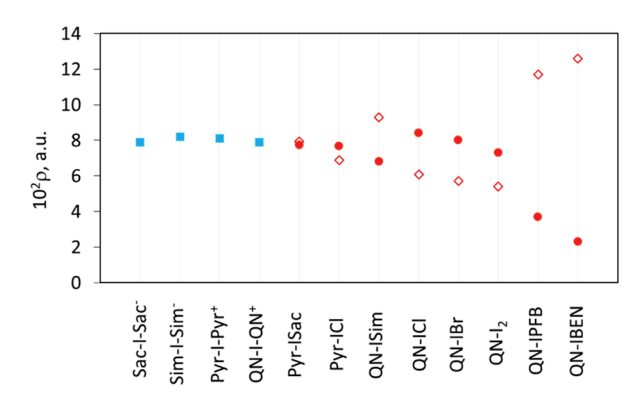


Figure 8. Electron density at BCP at  $N\cdots I$  bonds in halonium ions (blue squares) as well as  $N\cdots I$  (red circles) and  $I\cdots X$  (red rhombics) bonds in HaB complexes.

complexes. In the weaker complexes of QN with IPFB and IBEN, the values of  $\rho(\mathbf{r})$  at the I···N bond paths (about 0.04 and 0.02 a.u.) are 4–5 times lower than those at the corresponding I···X paths (the latter are close to 0.1 a.u., as expected for the fully developed covalent bonds).

The values of the energy density (Figure 9) showed the same trends as those of electron densities.

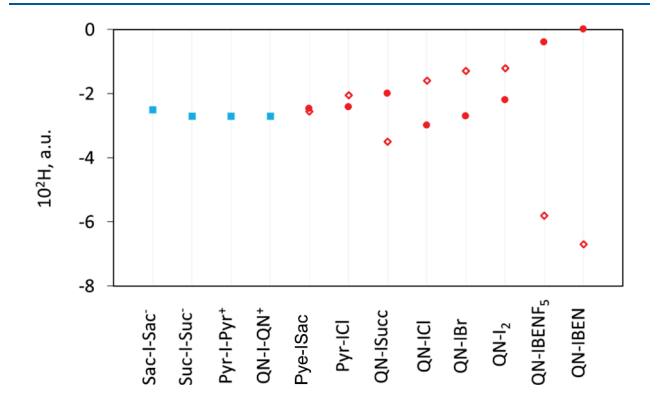


Figure 9. Energy density at BCP at N···I bonds in halonium ions (blue squares) as well as N···I (red circles) and I···X (red rhombics) bonds in HaB complexes.

Previous studies related the negative values of  $H(\mathbf{r})$  with the covalency of the corresponding bonds (and the rise of the

magnitude of these values reflects the increase of the contribution of the covalent component). To  $^{76,80}$  It is thus noticeable that the  $H(\mathbf{r})$  values at BCPs of the I···M bonds in the strong HaB complexes are negative and their magnitudes are comparable to those found for the I···X and I···N bonds in the halonium ions. In comparison, in the (moderately strong) complex of QN with IPFB, the magnitude of the negative H values is much smaller (indicating lower contributions of the covalent interactions). Furthermore, the very small and positive  $H(\mathbf{r})$  value in the QN·IBEN (Table S6 in the Supporting Information) is consistent with the predominantly electrostatic character of bonding in this complex.

Finally, the similarity (and covalent character) of the N···I and I···X interactions in the strong HaB complexes and their analogy to the bonding in halonium ions were verified by the DORI. Following the development of the NCI plots for the identification and visualization of noncovalent interactions, the DORI was designed for the simultaneous visualization of both covalent and noncovalent interactions. It reveals the density overlap regions (bonds, intermolecular interactions, and steric clashes) showing deviations from the exponential dependences and identifies interactions using the sign of the second eigenvalue of the density Hessian. The DORI representations of the complex of QN with IPFB (Figure 10) show a blue disk between the iodine atom and the QN molecule. Similar to NCI, such disks represent strong intermolecular bonding.

On the other hand, there is a dark blue cylinder between the iodine and the aromatic ring in QN·IPFB, which represents covalent bonds. Both anionic and cationic halonium ions show such cylinders between the central iodines and nitrogen atoms. The DORI representation of the strong complex formed by QN and IBr produced an analogous blue cylinder (indicating covalent bonding) along both the N···I and I···Br bonds, indicating their covalent character and their similarity to bonding in halonium ions.

#### 4. SUMMARY AND CONCLUSIONS

X-ray structural measurements and computational analysis demonstrated that the analogy between N···I···N bonding in (anionic and cationic) halonium ions and halogen X–I···N bonding in the associations formed by the strong HaB donors and acceptors extends beyond similar bond lengths and energies. Indeed, such halogen bonding is accompanied by

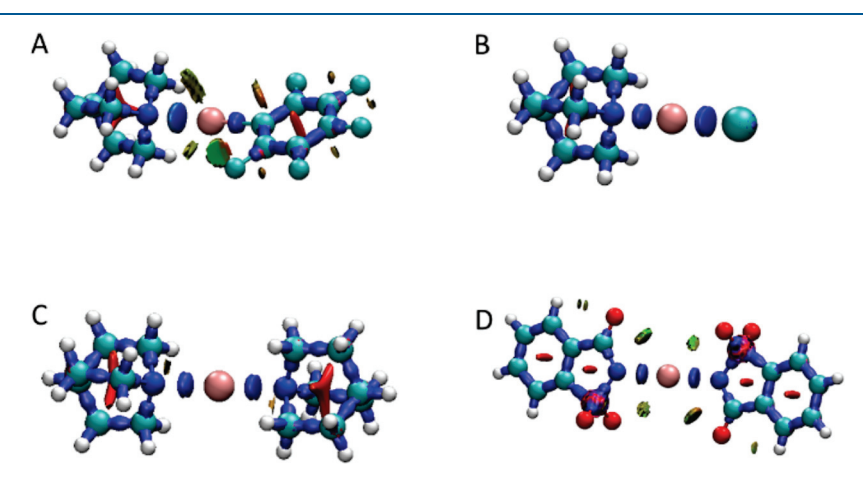


Figure 10. DORI representations of QN·IPFB (A), QN·IBr (B), QN·I·QN (C), and Sac·I·Sac (D).

considerable charge transfer and polarization of the HaB donor. This leads to a weakening of the I–X bond and a partial positive charge on the halogen-bonded iodine. As a result, such halogen bonding looks like the interaction of two electron donors (the Lewis basis), D and D', with a central iodonium cation. Thus, similar to halonium and trihalide ions, <sup>79</sup> these HaB complexes can be described by the MO diagram in Figure 1, right, with two distinct electron donors, D and D' (and somewhat different energy of their HOMOs).

The binding energies and MBO indices for both N···I and I...X bonds in the strong HaB complexes are comparable to those found for I···N bonds in the halonium ions. Their relative lengths and strengths apparently depend on the electron donor strength (or basicity) of D and D', and, in the solid state, on the effects of the environment. While in the majority of the HaB complexes, the I···X bond is stronger than the I···N bond, this relationship is reversed in some systems (e.g., the solid-state complex of ISac with 4-aminopyridine is characterized by the shorter N-I bond with pyridine than that with the saccharine residue, i.e., it can be presented as halogen bonding of a N-iodopyridinium cation with a saccharide anion<sup>40</sup>). As such, these HaB complexes represent asymmetric 3c-4e systems with the central atom shifted one way or another (it should be noted in this respect that the symmetry of the N-I-N bonding in the halonium cation is also frequently distorted by crystal forces, noncovalent bonding to one side, etc., 30,83,84).

The similarities of the X···I···N bonding in the strong HaB complexes and the N···I···N bonding in halonium ions are further supported by the very close electron densities and energies at BCPs for both N···I and I···X bonds in the HaB complexes and iodonium ions and by DORI analysis. Overall, all these data point out the analogy of the asymmetric (polarized) X···I···N bonding in the strong HaB complexes and (more or less) symmetric N···I···N bonding in the halonium cations and anions, which in all cases is best represented as a weak covalent interaction with a bond order of about 0.5. Finally, while the weaker HaB complexes are quite different from the strong ones discussed herein, they all appear as parts of the continuum of N···I (and other HaB 78,85) bonds (Figure S1 in the Supporting Information). Taken together with the other data, 43,86,87 this continuum indicates that all bonding properties are changing gradually and even moderately strong halogen bonding contains significant covalent component.

#### ASSOCIATED CONTENT

#### Supporting Information

The Supporting Information is available free of charge at https://pubs.acs.org/doi/10.1021/acs.inorgchem.3c02843.

Crystallographic, data collection, and structure refinement details; energies and atomic coordinates of the optimized species; interaction energies and EDA in solid-state complexes; I···N bond distribution from Cambridge Crystallographic Database; linear dependence of the calculated and experimental I···N bonds length and energies; NBO and AIM charges; MBO values; and electron and energy densities at BCPs (PDF)

#### **Accession Codes**

CCDC 2287815 - 2287818 contain the supplementary crystallographic data for this paper. These data can be obtained free of charge via www.ccdc.cam.ac.uk/data -

request/cif, or by emailing data\_request@ccdc.cam.ac.uk, or by contacting The Cambridge Crystallographic Data Centre, 12 Union Road, Cambridge CB2 1EZ, UK; fax: +44 1223 336033.

#### AUTHOR INFORMATION

#### **Corresponding Author**

Sergiy V. Rosokha — Department of Chemistry, Ball State University, Muncie, Indiana 47306, United States; orcid.org/0000-0003-3172-8523; Email: svrosokha@bsu.edu

#### **Authors**

Emmanuel Adeniyi – Department of Chemistry, Ball State University, Muncie, Indiana 47306, United States

Favour E. Odubo – Department of Chemistry, Ball State University, Muncie, Indiana 47306, United States

Matthias Zeller — Department of Chemistry, Purdue University, West Lafayette, Indiana 47907, United States; orcid.org/0000-0002-3305-852X

Yury V. Torubaev – Department of Chemistry, Ben-Gurion University of the Negev, Beer-Sheva 84105, Israel

Complete contact information is available at: https://pubs.acs.org/10.1021/acs.inorgchem.3c02843

#### Notes

The authors declare no competing financial interest.

#### ACKNOWLEDGMENTS

E.A., F.E.O., and S.V.R. thank the National Science Foundation (grant CHE-2003603) for financial support of this work. X-ray structural measurements were supported by the National Science Foundation through the Major Research Instrumentation Program under grant no. CHE 1625543 (funding for the single crystal X-ray diffractometer). Calculations were done on Ball State University's Beowulf cluster, which is supported by the National Science Foundation (MRI-1726017) and Ball State University.

#### **■ REFERENCES**

- (1) Metrangolo, P.; Resnati, G. Halogen bonding: a paradigm in supramolecular chemistry. *Chem.—Eur. J.* **2001**, *7*, 2511–2519.
- (2) Cavallo, G.; Metrangolo, P.; Milani, R.; Pilati, T.; Priimagi, A.; Resnati, G.; Terraneo, G. The halogen bond. *Chem. Rev.* **2016**, *116*, 2478–2601.
- (3) Gilday, L. C.; Robinson, S. W.; Barendt, T. A.; Langton, M. J.; Mullaney, B. R.; Beer, P. D. Halogen bonding in supramolecular chemistry. *Chem. Rev.* **2015**, *115*, 7118–7195.
- (4) Desiraju, G. R.; Ho, P. S.; Kloo, L.; Legon, A. C.; Marquardt, R.; Metrangolo, P.; Politzer, P.; Resnati, G.; Rissanen, K. Definition of the halogen bond (IUPAC Recommendations 2013). *Pure Appl. Chem.* 2013, 85, 1711–1713.
- (5) Pennington, W. T.; Hanks, T. W.; Arman, H. D. Halogen bonding with dihalogens and interhalogens. *Struct. Bonding (Berlin)* **2008**, *126*, 65–104.
- (6) Colin, M. M.; Gaultier de Claubry, H. Sur le combinaisons de l'iode avec les substances végétales et animales. *Ann. Chim.* **1814**, *90*, 87–100.
- (7) Benesi, H. A.; Hildebrand, J. H. A spectrophotometric investigation of the interaction of iodine with aromatic hydrocarbons. *J. Am. Chem. Soc.* **1949**, 71, 2703–2707.
- (8) Hassel, O.; Hvoslef, J.; Vihovde, E. H.; Sörensen, N. A. The structure of bromine 1,4-dioxanate. *Acta Chem. Scand.* **1954**, *8*, 873.
- (9) Mulliken, R. S. Molecular compounds and their spectra. II. J. Am. Chem. Soc. 1952, 74, 811–824.

- (10) Mulliken, R. S.; Person, W. B. Molecular Complexes. A Lecture and Reprint Volume; Wiley: New York, 1969.
- (11) Foster, R. Organic Charge-Transfer Complexes; Academic: New York, 1969.
- (12) Herbstein, F. H. Crystalline Molecular Complexes and Compounds: Structures and Principles; Oxford University Press: New York, 2005.
- (13) Politzer, P.; Murray, J. S.; Clark, T. Halogen bonding: an electrostatically-driven highly directional noncovalent interaction. *Phys. Chem. Chem. Phys.* **2010**, *12*, 7748–7757.
- (14) Prescott, A. B. The periodides. J. Am. Chem. Soc. 1895, 17, 775-781.
- (15) Pauling, L. The Nature of the Chemical Bond; Cornell University Press: Ithaca, NY, 1940.
- (16) Rundle, R. E. Electron deficient compounds1. J. Am. Chem. Soc. 1947, 69, 1327–1331.
- (17) Pimentel, G. C. The bonding of trihalide and bifluoride ions by the molecular orbital method. *J. Chem. Phys.* **1951**, *19*, 446–448.
- (18) Barluenga, J.; González, J. M.; Campos, P. J.; Asensio, G. I(Py)<sub>2</sub>BF<sub>4</sub>, a new reagent in organic synthesis: general method for the 1,2-iodofunctionalization of olefins. *Angew Chem. Int. Ed. Engl.* **1985**, 24 (4), 319–320.
- (19) Gong, G.; Lv, S.; Han, J.; Xie, F.; Li, Q.; Xia, N.; Zeng, W.; Chen, Y.; Wang, L.; Wang, J.; Chen, S. Halogen-bonded organic framework (XOF) based on iodonium-bridged N···I+···N interactions: a type of diphase periodic organic network. *Angew. Chem., Int. Ed.* **2021**, 60 (27), 14831–14835.
- (20) Vanderkooy, A.; Gupta, A. K.; Földes, T.; Lindblad, S.; Orthaber, A.; Pápai, I.; Erdélyi, M. Halogen bonding helicates encompassing iodonium cations. *Angew. Chem., Int. Ed.* **2019**, *58* (27), 9012–9016.
- (21) Maity, A.; Frey, B. L.; Powers, D. C. Iodanyl radical catalysis. *Acc. Chem. Res.* **2023**, *56* (14), 2026–2036.
- (22) Muñiz, K.; García, B.; Martínez, C.; Piccinelli, A. Dioxoiodane compounds as versatile sources for iodine(I) chemistry. *Chem.—Eur. J.* 2017, 23 (7), 1539–1545.
- (23) Turunen, L.; Erdélyi, M. Halogen bonds of halonium ions. Chem. Soc. Rev. 2020, 49, 2688–2700.
- (24) Ebrahimi, A.; Razmazma, H.; Delarami, H. S. The nature of halogen bonds in [N···X···N]+ complexes: a theoretical study. *Phys. Chem. Res.* **2016**, *4*, 1–15.
- (25) Hakkert, S. B.; Erdélyi, M. halogen bond symmetry:the N-X-N bond. J. Phys. Org. Chem. 2015, 28, 226–233.
- (26) Karim, A.; Reitti, M.; Carlsson, A.-C. C.; Gräfenstein, J.; Erdélyi, M. The nature of [N-Cl-N]+ and [N-F-N]+ halogen bonds in solution. *Chem. Sci.* **2014**, *5*, 3226–3233.
- (27) Velasquez, J. D.; Echeverría, J.; Alvarez, S. Structure and bonding of halonium compounds. *Inorg. Chem.* **2023**, *62*, 8980–8992.
- (28) Koskinen, L.; Hirva, P.; Kalenius, E.; Jääskeläinen, S.; Rissanen, K.; Haukka, M. Halogen bonds with coordinative nature: halogen bonding in a S-I\*-S iodonium complex. *CrystEngComm* **2015**, *17*, 1231–1236.
- (29) Georgiou, D. C.; Butler, P.; Browne, E. C.; Wilson, D. J. D.; Dutton, J. L. On the Bonding in Bis-pyridine Iodonium Cations. *Aust. J. Chem.* **2013**, *66*, 1179–1188.
- (30) Yu, S.; Truong, K.-N.; Siepmann, M.; Siiri, A.; Schumacher, C.; Ward, J. S.; Rissanen, K. Halogen-bonded [N-I-N]<sup>-</sup> complexes with symmetric or asymmetric three-center-four-electron bonds. *Cryst. Growth Des.* **2023**, 23 (2), 662–669.
- (31) Clark, T.; Murray, J. S.; Politzer, P. The sigma-hole Coulombic intyrepretation of trihalide anion formation. *ChemPhysChem* **2018**, *19*, 3044–3049.
- (32) Peuronen, A.; Valkonen, A.; Kortelainen, M.; Rissanen, K.; Lahtinen, M. Halogen bonding-based "catch and release": reversible solid-state entrapment of elemental iodine with monoalkylated DABCO salts. *Cryst. Growth Des.* **2012**, *12*, 4157–4169.
- (33) Aghabali, A.; Jun, S.; Olmstead, M. M.; Balch, A. L. Piperazine-functionalized  $C_{60}$  and diiodine or iodine monochloride as

- components in forming supramolecular assemblies. *Dalton Trans.* **2017**, *46*, 3710–3715.
- (34) Borley, W.; Watson, B.; Nizhnik, Y.; Zeller, M.; Rosokha, S. V. Complexes of diiodine with heteroaromatic N-oxides: effects of halogen-bond acceptors in halogen bonding. *J. Phys. Chem. A* **2019**, 123, 7113–7123.
- (35) Torubaev, Y. V.; Howe, D.; Leitus, G.; Rosokha, S. V. The relationship between the crystal habit and the energy framework pattern: a case study involving halogen bonding on the edge of a covalent bond. *CrystEngComm* **2023**, 25 (23), 3380–3390.
- (36) Yu, S.; Ward, J. S. Ligand exchange among iodine(I) complexes. *Dalton Trans.* **2022**, *51*, 4668–4674.
- (37) Guzmán Santiago, A. J.; Brown, C. A.; Sommer, R. D.; Ison, E. A. Identification of key functionalization species in the Cp\*Ir(III)-catalyzed-ortho halogenation of benzamides. *Dalton Trans.* **2020**, 49 (45), 16166–16174.
- (38) Ward, J. S.; Fiorini, G.; Frontera, A.; Rissanen, K. Asymmetric [N-I-N]<sup>+</sup> halonium complex. *Chem. Commun.* **2020**, *56*, 8428–8431.
- (39) Raatikainen, K.; Rissanen, K. Interaction between amines and N-haloimides: a new motif for unprecedentedly short Br... N and I... N halogen bonds. *CrystEngComm* **2011**, *13*, 6972–6977.
- (40) Makhotkina, O.; Lieffrig, J.; Jeannin, O.; Fourmigué, M.; Aubert, E.; Espinosa, E. Cocrystal or salt: solid state-controlled iodine shift in crystalline halogen-bonded systems. *Cryst. Growth Des.* **2015**, 15 (7), 3464–3473.
- (41) Eraković, M.; Nemec, V.; Lež, T.; Porupski, I.; Stilinović, V.; Cinčić, D. Halogen bonding of N-bromophthalimide by grinding and solution crystallization. *Cryst. Growth Des.* **2018**, *18* (2), 1182–1190.
- (42) Nakanishi, W.; Hayashi, S.; Kihara, H. On the stability and the bonding Model of  $N\rightarrow\sigma^*$  type molecular complexes, R2Z-X-X: Proposal of 3c-4e description for Z-X-X in the adducts. *J. Org. Chem.* **1999**, *64* (8), 2630–2637.
- (43) Oliveira, V.; Kraka, E.; Cremer, D. The intrinsic strength of the halogen bond: electrostatic and covalent contributions described by coupled cluster theory. *Phys. Chem. Chem. Phys.* **2016**, *18* (48), 33031–33046.
- (44) Oliveira, V.; Kraka, E.; Cremer, D. Quantitative assessment of halogen bonding using vibrational spectroscopy. *Inorg. Chem.* **2017**, *56*, 488–502.
- (45) Li, D.; Xia, T.; Feng, W.; Cheng, L. Revisiting the covalent nature of halogen bonding: a polarized three-center four-electron bond. *RSC Adv.* **2021**, *11* (52), 32852–32860.
- (46) Ward, J. S.; Frontera, A.; Rissanen, K. Iodonium complexes of the tertiary amines quinuclidine and 1-ethylpiperidine. *Dalton Trans.* **2021**, *50*, 8297–8301.
- (47) Li, J.; Kwon, E.; Lear, M. J.; Hayashi, Y. Halogen bonding of N-halosuccinimides with amines and effects of brønsted acids in quinuclidine-catalyzed halocyclizations. *Helv. Chim. Acta* **2021**, *104* (9), No. e2100080.
- (48) Bruker Apex3 v2016.9-0, SAINT V8.37A; Bruker AXS Inc.: Madison, WI, 2016.
- (49) Krause, L.; Herbst-Irmer, R.; Sheldrick, G. M.; Stalke, D. Comparison of silver and molybdenum microfocus X-ray sources for single-crystal structure determination. *J. Appl. Crystallogr.* **2015**, 48, 3–10.
- (50) Hübschle, C. B.; Sheldrick, G. M.; Dittrich, B. ShelXle: A Qt Graphical User Interface for SHELXL. *J. Appl. Crystallogr.* **2011**, 44, 1281–1284.
- (51) Sheldrick, G. M. Crystal structure refinement with SHELXL. Acta Crystallogr., Sect. C: Struct. Chem. 2015, 71 (1), 3-8.
- (52) Frisch, M. J.; Trucks, G. W.; Schlegel, H. B.; Scuseria, G. E.; Robb, M. A.; Cheeseman, J. R.; Scalmani, G.; Barone, V.; Mennucci, B.; Petersson, G. A.; Nakatsuji, H.; Caricato, M.; Li, X.; Hratchian, H. P.; Izmaylov, A. F.; Bloino, J.; Zheng, G.; Sonnenberg, J. L.; Hada, M.; Ehara, M.; Toyota, K.; Fukuda, R.; Hasegawa, J.; Ishida, M.; Naka Jima, T.; Honda, Y.; Kitao, O.; Nakai, H.; Vreven, T.; Montgomery, J. A., Jr.; Peralta, J. E.; Ogliaro, F.; Bearpark, M.; Heyd, J. J.; Brothers, E.; Kudin, K. N.; Staroverov, V. N.; Kobayashi, R.; Nor-Mand, J.; Raghavachari, K.; Rendell, A.; Burant, J. C.; Iyengar, S. S.; Tomasi, J.;

- Cossi, M.; Rega, N.; Millam, J. M.; Klene, M.; Knox, J. E.; Cross, J. B.; Bakken, V.; Adamo, C.; Jaramillo, J.; Gomperts, R.; Strat-Mann, R. E.; Yazyev, O.; Austin, A. J.; Cammi, R.; Pomelli, C.; Ochter-Ski, J. W.; Martin, R. L.; Morokuma, K.; Zakrzewski, V. G.; Voth, G. A.; Salvador, P.; Dannenberg, J. J.; Dapprich, S.; Daniels, A. D.; Farkas, O.; Foresman, J. B.; Ortiz, J. V.; Cioslowski, J.; Fox, D. J. *Gaussian 09*, Revision C.01; Gaussian, Inc.: Wallingford CT, 2009.
- (53) Zhao, Y.; Truhlar, D. G. The M06 suite of density functionals for main group thermochemistry, thermochemical kinetics, non-covalent interactions, excited states, and transition elements: two new functionals and systematic testing of four M06-class functionals and 12 other functionals. *Theor. Chem. Acc.* 2008, 120, 215–241.
- (54) Weigend, F.; Ahlrichs, R. Balanced basis sets of split valence, triple zeta valence and quadruple zeta valence quality for H to Rn: design and assessment of accuracy. *Phys. Chem. Chem. Phys.* **2005**, 7 (18), 3297–3305.
- (55) Tomasi, J.; Mennucci, B.; Cammi, R. Quantum mechanical continuum solvation models. *Chem. Rev.* **2005**, *105*, 2999–3094.
- (56) Zhu, Z.; Xu, Z.; Zhu, W. Interaction nature and computational methods for halogen bonding: a perspective. *J. Chem. Inf. Model.* **2020**, *60*, 2683–2696.
- (57) Bauzá, A.; Alkorta, I.; Frontera, A.; Elguero, J. On the reliability of pure and hybrid dft methods for the evaluation of halogen, chalcogen, and pnicogen bonds involving anionic and neutral electron donors. *J. Chem. Theory Comput.* **2013**, 9 (11), 5201–5210.
- (58) Weinhold, F.; Landis, C. R. Discovering Chemistry with Natural Bond Orbitals; Wiley: Hoboken, NJ, 2012.
- (59) Bader, R. F. W. A Quantum theory of molecular structure and its applications. *Chem. Rev.* **1991**, *91*, 893–928.
- (60) de Silva, P.; Corminboeuf, C. Simultaneous visualization of covalent and noncovalent interactions using regions of density overlap. *J. Chem. Theory Comput.* **2014**, *10*, 3745–3756.
- (61) Mayer, I. Bond order and valence indices: A personal account. *J. Comput. Chem.* **2007**, 28 (1), 204–221.
- (62) Bridgeman, A. J.; Cavigliasso, G.; Ireland, L. R.; Rothery, J. The Mayer bond order as a tool in inorganic chemistry. *J. Chem. Soc., Dalton Trans.* **2001**, 2095–2108.
- (63) Lu, T.; Chen, F. Multiwfn: a multifunctional wavefunction analyzer. J. Comput. Chem. 2012, 33, 580-592.
- (64) Humphrey, W.; Dalke, A.; Schulten, K. VMD Visual Molecular Dynamics. *J. Mol. Graphics* 1996, 14, 33–38.
- (65) Spackman, P. R.; Turner, M. J.; McKinnon, J. J.; Wolff, S. K.; Grimwood, D. J.; Jayatilaka, D.; Spackman, M. A. *CrystalExplorer*: a program for Hirshfeld surface analysis, visualization and quantitative analysis of molecular crystals. *J. Appl. Crystallogr.* **2021**, *54*, 1006–1011.
- (66) Mackenzie, C. F.; Spackman, P. R.; Jayatilaka, D.; Spackman, M. A. CrystalExplorer model energies and energy frameworks: extension to metal coordination compounds, organic salts, solvates and open-shell systems. *IUCrJ* 2017, 4 (5), 575–587.
- (67) Otte, F.; Kleinheider, J.; Hiller, W.; Wang, R.; Englert, U.; Strohmann, C. Weak yet decisive: molecular halogen bond and competing weak interactions of iodobenzene and quinuclidine. *J. Am. Chem. Soc.* **2021**, *143* (11), 4133–4137.
- (68) Dolenc, D.; Modec, B. EDA Complexes of N-halosaccharins with N- and O-donor ligands. *New J. Chem.* **2009**, 33 (11), 2344–2349.
- (69) Jones, R. H.; Knight, K. S.; Marshall, W. G.; Clews, J.; Darton, R. J.; Pyatt, D.; Coles, S. J.; Horton, P. N. Colossal thermal expansion and negative thermal expansion in simple halogen bonded complexes. *CrystEngComm* **2014**, *16* (2), 237–243.
- (70) Dahl, T.; Hassel, O.; Sky, K.; Nilsson, Å.; Theorell, H.; Blinc, R.; Paušak, S.; Ehrenberg, L.; Dumanović, J. Structure of complexes formed by pyridine with cyanogen iodide and iodine bromide. *Acta Chem. Scand.* **1967**, *21*, 592–593.
- (71) Tuikka, M.; Haukka, M. Crystal structure of the pyridine-diiodine (1/1) adduct. *Acta Crystallogr., Sect. E: Crystallogr. Commun.* **2015**, 71, 0463.

- (72) Okitsu, T.; Yumitate, S.; Sato, K.; In, Y.; Wada, A. Substituent effect of bis(pyridines)iodonium complexes as iodinating reagents: control of the iodocyclization/oxidation process. *Chem.—Eur. J.* **2013**, 19, 4992–4996.
- (73) Bondi, A. van der Waals volumes and radii. *J. Phys. Chem.* **1964**, 68, 441–451.
- (74) Conquest Version 2022.3.0. Cambridge Crystallographic Data Centre, 2022.
- (75) Matta, C. F., Boyd, R. J., Eds. Quantum Theory of Atoms in Molecules, from Solid State to DNA and Drug Design; Wiley VCH: Weinheim, 2007.
- (76) Popelier, P. L. A. The QTAIM perspective of chemical bonding. In *The Chemical Bond*; John Wiley & Sons, Ltd, 2014; p 271.
- (77) Espinosa, E.; Alkorta, I.; Elguero, J.; Molins, E. From weak to strong interactions: a comprehensive analysis of the topological and energetic properties of the electron density distribution involving X-H···F-Y systems. *J. Chem. Phys.* **2002**, *117*, 5529–5542.
- (78) Miller, D. K.; Loy, C.; Rosokha, S. V. Examining a transition from supramolecular halogen bonding to covalent bonds: topological analysis of electron densities and energies in the complexes of bromosubstituted electrophiles. ACS Omega 2021, 6, 23588–23597.
- (79) Nakanishi, W.; Hayashi, S.; Narahara, K. Polar coordinate representation of  $H_b(r_c)$  versus  $(h^2/8m)(^2(r_c)$  at BCP in AIM analysis: classification and evaluation of weak to strong interactions. *J. Phys. Chem. A* **2009**, *113*, 10050–10057.
- (80) Cremer, D.; Kraka, E. A Description of the chemical bond in terms of local properties of electron density and energy. *Croat. Chem. Acta* 1984, 57, 1259–1281.
- (81) Miller, D. K.; Chernyshov, I. Y.; Torubaev, Y. V.; Rosokha, S. V. From weak to strong interactions: structural and electron topology analysis of the continuum from the supramolecular chalcogen bonding to covalent bonds. *Phys. Chem. Chem. Phys.* **2022**, 24, 8251–8259.
- (82) Johnson, E. R.; Keinan, S.; Mori-Sánchez, P.; Contreras-García, J.; Cohen, A. J.; Yang, W. Revealing Noncovalent Interactions. *J. Am. Chem. Soc.* **2010**, *132*, 6498–6506.
- (83) Svensson, P. H.; Kloo, L. Synthesis, structure, and bonding in polyiodide and metal iodide-iodine systems. *Chem. Rev.* **2003**, *103*, 1649–1684.
- (84) Reiersølmoen, A. C.; Battaglia, S.; Øien-Ødegaard, S.; Gupta, A. K.; Fiksdahl, A.; Lindh, R.; Erdélyi, M. Symmetry ofthree-center, four-electron bonds. *Chem. Sci.* **2020**, *11*, 7979–7990.
- (85) Weinberger, C.; Hines, R.; Zeller, M.; Rosokha, S. V. Continuum of covalent to intermolecular bonding in the halogenbonded complexes of 1,4-diazabicyclo[2.2.2]octane with bromine-containing electrophiles. *Chem. Commun.* **2018**, *54*, 8060–8063.
- (86) Robinson, S. W.; Mustoe, C. L.; White, N. G.; Brown, A.; Thompson, A. L.; Kennepohl, P.; Beer, P. D. Evidence for halogen bond covalency in acyclic and interlocked halogen-bonding receptor anion recognition. *J. Am. Chem. Soc.* **2015**, *137*, 499–507.
- (87) Kellett, C. W.; Kennepohl, P.; Berlinguette, C. P.  $\pi$ -Covalency in the halogen bond. *Nat. Commun.* **2020**, *11*, 3310.